HAL
archives-ouvertes.fr

Geodesic Image Normalization in the Space of Diffeomorphisms

Brian Avants, C.L. Epstein, James C. Gee

▶ **To cite this version:**

Brian Avants, C.L. Epstein, James C. Gee. Geodesic Image Normalization in the Space of Diffeomorphisms. Xavier Pennec and Sarang Joshi. 1st MICCAI Workshop on Mathematical Foundations of Computational Anatomy: Geometrical, Statistical and Registration Methods for Modeling Biological Shape Variability, Oct 2006, Copenhagen, Denmark. pp.125-135, 2006. <inria-00636082>

HAL Id: inria-00636082
https://hal.inria.fr/inria-00636082

Submitted on 26 Oct 2011

HAL is a multi-disciplinary open access archive for the deposit and dissemination of scientific research documents, whether they are published or not. The documents may come from teaching and research institutions in France or abroad, or from public or private research centers.

L'archive ouverte pluridisciplinaire **HAL**, est destinée au dépôt et à la diffusion de documents scientifiques de niveau recherche, publiés ou non, émanant des établissements d'enseignement et de recherche français ou étrangers, des laboratoires publics ou privés.

Geodesic Image Normalization in the Space of Diffeomorphisms

Brian B. Avants and C. L. Epstein and J. C. Gee

Depts. of Radiology and Mathematics,
University of Pennsylvania
Philadelphia, PA 19101

Abstract. Quantitative, deformable mappings between images are increasingly important as measurement tools in biology and medicine. The theory of diffeomorphisms (smooth differentiable bijections with differentiable inverse) provides a mathematical foundation for the computation and interpretation of these maps. Miller, in particular, has used this theory to develop image normalization techniques that rely on a distance measurement as a regularizer. Here, we use this metric within a general transformation framework that explicitly parameterizes the image to image mapping as a symmetric geodesic path in the space of diffeomorphisms. The key difference between our approach and Miller's is that ours does not choose a single end-point (or template image) from which to measure the map. Rather, we search for the shortest diffeomorphism (smallest deformation) between images by optimizing the transformation with respect to both of its end-points. This algorithm, geodesic normalization, provides solutions that are invariant to which of the input coordinate systems (images) is chosen as a reference. This allows the method to compute metric distances, have truly symmetric performance and to give full space-time solutions that are invertible and diffeomorphic in the discrete domain. Finally, our algorithm guarantees that our solutions and their inverses are consistent to a sub-pixel level.

1 Introduction

Computational anatomy (CA) uses imaging to make quantitative measurements of the natural world. One may view CA as the science of biological shape and its variation, with roots in the work of Charles Darwin and D'Arcy Thompson [1, 2]. The wide availability of high resolution *in vivo* functional and structural imaging has caused a rapid increase in CA's relevance and prominence. Currently, this developing science's primary tools are the topology preserving diffeomorphic transformations. These transformations are used to map an individual image J into the space of a template image, $\bar{I}$, which serves as a common coordinate system. When a population of images is mapped together by these transformations, each voxel in individual space corresponds smoothly with a single voxel in the reference space. This process creates a continuous spatial map of population

information detailing, for example, the relative volume, functional activation or diffusion at a given anatomical position, such as the anterior hippocampus or occipital lobe gray matter. Topology preserving transformation (TPT) are of special interest for this technology as they will introduce neither folds nor tears in this map and will preserve the continuity of curves and surfaces.

Topology preserving normalization permits comparisons to be made across time points in an individual's disease process or to study development patterns across a large population [3–6]. Miller, et al. showed that Large Deformation Diffeomorphic Metric Matching (LDDMM) is able to localize hippocampal activation to provide increased statistical significance in functional imaging studies [7]. Avants et al used a Lagrangian diffeomorphic normalization technique to map and statistically differentiate functionally homologous structures between species [8]. Furthermore, large deformation mappings are better able to separate structural and signal (intensity) differences in population studies, particularly in the presence of atrophy or high shape variation. Diffeomorphic methods may also be extended to normalize vector or tensor images [9].

The CA studies cited above were enabled by recently developed, theoretically well-founded methods for studying topology preserving variation. The major advancement in this aspect of CA technology is to base the work in the space of diffeomorphisms. The diffeomorphic space is the broadest smooth, topology preserving space and allows one to very accurately capture both large and small deformation differences in shape. The collection of these transformations forms a mathematical group. Grenander [10], Mumford [11], Miller [12], Trouve [13] and Younes [14] have studied this group space in the context of computer vision and deformable image transformation and have derived Euler-Lagrange equations for CA [15].

Our approach to image normalization is based upon Arnol'd's definition of a symmetric, time-parameterized *shortest path* (geodesic) between two diffeomorphic configurations of a domain [16]. We argue that this view is fundamental to the theoretical foundation of diffeomorphic normalization, essential for computing true metric distances and desirable for its symmetry properties. Our algorithm will satisfy desirable continuity, anonymity and unanimity conditions [17] as well as the metric measurement properties needed for geodesics. This yields a new algorithm, geodesic normalization (GN), that parameterizes the deformation between an image pair with respect both ends of a geodesic path.

2 Mathematical Background on Diffeomorphisms

We now discuss some basic facts from the theory of diffeomorphisms, the mathematical underpinnings of GN. This section is derived from Arnol'd [18] and Marsden and Ratiu [19]. In this section, we will refer to ϕ as a geodesic in the space of diffeomorphisms and ϕ_1 and ϕ_2 as the components of ϕ, as described below. We also assume that the images and velocity fields referred to below are sufficiently differentiable and that we are only interested in transformations that visibly change the image. For example, a diffeomorphism of a constant image will

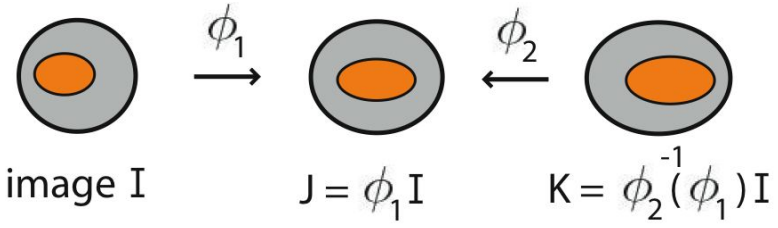

Fig. 1. A diffeomorphism is used to map image I into image J (left to center) via coordinate transformation. Composing two diffeomorphisms ϕ_1 and the inverse of ϕ_2 enables us to use the maps from K to J and from I to J to make a coordinate transformation from I to K.

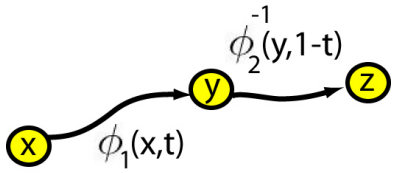

Fig. 2. An illustration of the geodesic path taken, in time, by the particle at position $\mathbf{x}$ in domain Ω. The path is geodesic if the diffeomorphism associated with the domain minimizes the distance metric in equation 2. The geodesic, ϕ is the whole path. Its points are traversed via ϕ_1 and ϕ_2.

be reduced to the identity. Image differentiability is required for the derivative computations necessary in the normalization method. Velocity field regularity guarantees the integrability necessary for generating diffeomorphisms. Typically, convolution with a Gaussian ensures image differentiability while a linear operator, L, induces sufficient smoothness on the velocity field. See Dupuis [20] for a discussion of regularity requirements on images and velocity field and the well-posedness given by diffeomorphic regularization.

Recall that a diffeomorphism is a smooth one-to-one and onto map with a smooth inverse. We always index diffeomorphisms with a spatial coordinate ($\mathbf{x}$, $\mathbf{y}$ or $\mathbf{z}$) and, if necessary, a time variable, t. However, we drop the spatial and temporal indexes for brevity where the meaning is clear. We define the diffeomorphic operations that we need as,

1. Coordinate transformation: this operation changes the coordinate system in which an object (image, vector field) is represented. The operation ϕI transforms the image $I(\mathbf{x})$ into the deformed image $\tilde{I}(\mathbf{y}) = I(\phi(\mathbf{x}, t))$ where the intensity $I(\mathbf{x})$ is equivalent to the intensity $\tilde{I}(\mathbf{y})$. We may also apply this operation to vector (or velocity) fields.
2. Transformation composition: this operation links diffeomorphisms together, generating a new map via $\phi_2(\phi_1(\mathbf{x}, t_1), t_2)$.

Understanding these operations are essential in image normalization. We illustrate them in figure 1.

Families of diffeomorphisms can be generated by integrating time-dependent velocity (vector) fields through an ordinary differential equation [18],

$$\frac{d\phi(\mathbf{x},t)}{dt} = \boldsymbol{V}(\mathbf{x},t). \tag{1}$$

This differential equation defines the change of the map, ϕ, by the value of a velocity field which is a smooth vector field. Velocities tell us how particles are moving through space: $\boldsymbol{V}$ assigns motion to a specific material point while $\boldsymbol{v}$ defines motion in a fixed coordinate system. The $\boldsymbol{V}$ in equation 1 is a *material velocity* in the Lagrangian frame. The *spatial velocity* is computed at the tangent space to the diffeomorphism at time, t, such that $\boldsymbol{v}(\mathbf{y},t) = \boldsymbol{V}(\mathbf{x},t)$ where the change in coordinates is indicated by the use of $\mathbf{x}$ in $\boldsymbol{V}$ and $\mathbf{y}$ in $\boldsymbol{v}$. We may also explicitly indicate the change in coordinates by using the map between the two coordinate systems, denoted by $\phi(\mathbf{x},t) = \mathbf{y}$, with inverse $\phi^{-1}(\mathbf{y},t) = \mathbf{x}$. Then, $\boldsymbol{V}(\mathbf{x},t) = \boldsymbol{v}(\phi(\mathbf{x}),t)$.

Deformable diffeomorphisms commonly used in image registration map domain Ω to itself. The map at the boundary, $\partial\Omega$, may also be defined as the identity, $\phi(\partial\Omega) = \partial\Omega$. This boundary constraint assumes that rigid motion has been factored out of the transformation between images. It also guarantees the transformation is everywhere one-to-one and onto and restricts the solution space to the diffeomorphic subgroup, $\mathcal{G}_0$.

$\mathcal{G}_0$ is a Frechet Lie group [21] when $\mathcal{G}_0$ is C^∞. The length of a diffeomorphic path between elements in this space is similar to the length of a curve, $\mathcal{C}$, connecting two points in Euclidean space, $l(\mathcal{C}) = \int_0^1 \|d\mathcal{C}/dt\|dt$, where the Euclidean length of the curve's tangent vector is integrated over its parameterization. Distances in the space of diffeomorphisms are infinite-dimensional analogies of curve length, where the infinitesimal increment in distance is given by a Sobolev norm, $\|\cdot\|$, operating on the tangent to the diffeomorphism (the spatial velocity) [20]. A *geodesic* between ψ_1 and ψ_2, two elements of $\mathcal{G}_0$, is defined by taking the infimum over all such paths [15],

$$D(\phi(0),\phi(1)) = \inf_{\phi} \int_0^1 \|\boldsymbol{v}(\phi(\mathbf{x},t))\|_L dt, \tag{2}$$
$$\phi(0) = \psi_1 \text{ and } \phi(1) = \psi_2,$$

where $\|\cdot\|_L$ is the Sobolev norm with respect to linear operator, L. Taking the infimum guarantees that we have a geodesic between the elements in $\mathcal{G}_0$. The length of the geodesic gives a metric distance, does not depend on the origin of its measurement (it has right invariance) and is the basis for GN as well as Miller, Trouve and Younes's work.

A geodesic in the space of diffeomorphisms thus defines the shortest route between two diffeomorphic transformations. Each transformation defines a single, unique configuration of the coordinate system. The length of the path itself is (trivially) symmetric, that is, $D(\phi(0),\phi(1)) = D(\phi(1),\phi(0)$ and satisfies metric properties. Furthermore, for all time $t \in [0,1]$, we have $\phi_2^{-1}(\phi_1(\mathbf{x},t),1-t) = \phi_1(\mathbf{x},1) = \mathbf{z}$. Rearranging this equation, we gain intermediate points along the

geodesic from $\phi_2(\mathbf{z}, 1-t) = \phi_2(\phi_1(\mathbf{x}, 1), 1-t) = \phi_1(\mathbf{x}, t)$. In this way, we see that *points along the geodesic are parameterized equivalently from coordinates at either end-point*. We will now introduce this coordinate system invariant parameterization into our normalization technology.

3 Geodesic Image Normalization

The goal of image registration, in general, is to find, for each $\mathbf{x}$ in I, the $\mathbf{z}$ in J that gives $I(\mathbf{x}) = J(\mathbf{z})$ or, alternatively, $f(J(\mathbf{z}))$ where f is an intensity-space transformation. If f is the identity, then the intensity at $\mathbf{x}$ in I should be equivalent to the intensity from coordinate $\mathbf{z}$ in J. The mapping from $\mathbf{x}$ to $\mathbf{z}$ may be written $\phi(\mathbf{x}) = \mathbf{z}$, from image I to image J such that points in I are in one-to-one correspondence with points in J.

When such maps are diffeomorphisms, we include a time parameter, t, that indexes the temporal evolution of ϕ. We refer to coordinates $\mathbf{x}$ in the time zero I domain, $\mathbf{z}$ in the time zero J domain and $\mathbf{y}$ in a common coordinate system that moves along the curve connecting $I(\mathbf{x})$ and $J(\mathbf{z})$. If this curve is a geodesic, then it is symmetric and will follow the same path whether starting from I or J. This symmetry means our time parameterized maps may be viewed from either endpoint at I or J such that $\phi_1(\mathbf{x}, t) = \mathbf{y} = \phi_2(\mathbf{z}, 1-t)$. This formulation allows us to deform I and J such that, for any $t \in [0,1]$ $I(\phi_1(\mathbf{x}, t)) = J(\phi_2(\mathbf{z}, 1-t))$. Such a motion gives a dense map in both space and time and is shown in figure 2 for one point in the image domain. The total mapping between the images is gained through the composition of these two components, $\phi(\mathbf{x}, 1) = \phi_2^{-1}(\phi_1(\mathbf{x}, t), 1-t)$. GN will exploit this geodesic view to gain symmetry. The algorithm will thus be able to compute the distance between two images, whereas previous algorithms computed asymmetric distance (not symmetric, therefore not a metric distance), due to a biased gradient descent approach that originates in a parameterization of the geodesic with respect to only one endpoint.

Let us now consider the case when we are given two images, I and J, of the same class, known to be (approximately) diffeomorphic. Here, we know neither the path in time nor which image should be considered as the template or reference image. We make the identification of $I(0)$ with I and $I(1)$ with J. We now seek to find the shortest diffeomorphism between these images such that $\phi_1(t)I = \phi_2(1-t)J$.

We now translate this example into a variational optimization problem. The variational energy for geodesic normalization therefore seeks ϕ_1 and ϕ_2 in order to locate the geodesic connecting I and J. Then, $\phi_1(\mathbf{x}, t)I = \phi_2(\mathbf{z}, 1-t)J$, gives the similarity term, $|\phi_1(t)I - \phi_2(1-t)J|^2$. The forward and backward energy is

then, using t as a parameter and solving to time $t = \bar{t}$,

$$E_{GN}(I,J) = \inf_{\phi_1} \inf_{\phi_2} \int_{t=0}^{\bar{t}} \omega\{ \|\boldsymbol{v}_1\|_L^2 + \|\boldsymbol{v}_2\|_L^2\}dt + \int_\Omega |\phi_1(\bar{t})I - \phi_2(1-\bar{t})J|^2 d\Omega. \quad (3)$$

Subject to:

each $\phi_i \in \mathcal{G}_0$ the solution of:

$$d\phi_i/dt = \boldsymbol{v}_i(\phi_i(t)) \text{ with } \phi_i(0) = \mathbf{Id}. \quad (4)$$

Minimization with respect to ϕ_1 and ϕ_2, upholding the arc length constraint, provides the *geodesic normalization*. Landmarks may also be included in this energy, as in our previous work [8], by dividing the similarity term, as done with the image match terms above. A similar image matching equation appeared in [22] and [23] as part of a derivation for template generation.

Once this problem is solved, the total symmetric normalization transformation from I to J is $\phi_1(\mathbf{x},1) = \phi_2^{-1}(\phi_1(\mathbf{x},0.5),0.5)$ and from J to I, $\phi_2(\mathbf{z},1) = \phi_1^{-1}(\phi_2(\mathbf{z},0.5),0.5)$. This is distinct from inverse consistent image registration [24] in which a variational term is used to estimate "inverse consistency" and symmetry and invertibility are not guaranteed. The inverse consistency is inherent to our method and is shown for synthetic data in figure 3 and for real data in figure 4. The algorithm is useful for generating shape means as well as symmetric geodesic image interpolation, formulated in [25].

We will show below that the maps computed by this algorithm satisfy Eckmann's continuity, symmetry (anonymity) and unanimity conditions. Eckmann and Weinberger discuss the existence of such maps [17, 26] and note the connection with the *generalized mean*. Denote a symmetric map, ϕ, connecting I and J. Eckmann's properties, adapted for image normalization, are then

1. Continuity: the map should vary continuously with the inputs I, J.
2. Symmetry / Anonymity: ϕ does not depend on permutations of I, J. This is verified if $\mathcal{A}(I,J) = \phi$ then $\mathcal{A}(J,I) = \phi^{-1}$.
3. Unanimity [17]: the map should output $\phi = \mathbf{Id}$ if $I = J$.

A map that violates anonymity (2 above) is labeled asymmetric. We now argue that GN satisfies the three conditions given above.

Theorem 1. *The solutions, $\phi_1(\mathbf{x},t)$ and $\phi_2(\mathbf{y},s)$, found by GN satisfy the three generalized mean axioms above.*

Continuity. Continuity was shown in Dupuis's proof of well-posedness for the diffeomorphic variational image matching problem [20]. As our problem is, in a global sense, identical, continuity is inherited.

Unanimity. The unanimity condition is also satisfied as all velocities will be $\mathbf{0}$ if all images are identical.

Anonymity. We prove anonymity by simply checking that permuting the labels in the variational energy produces an identical optimization problem, which

visual inspection confirms. Furthermore, the Euler-Lagrange equations depend symmetrically on gradients of both I and J. ■.

Geodesic Normalization Implementation: Algorithm 1 states the locally optimal GN algorithm without landmarks, as described in previous sections. A similar approach can be used for landmark matching. The input to the algorithm is a pair of images and a user set number of time interpolation points, $\{t_i\}$, where $t_0 = 0$ and $t_n = 0.5$ and n is even. The output is ϕ_1, ϕ_2 defined on $\Omega \times [0, 0.5]$ and their inverses. These define the full ϕ_i mappings and their inverses at (deformation) time 1.

Algorithm 1 : Geodesic Normalization (GN)

The algorithm notation is the same as in the body of the paper. We compute ϕ_1^{-1} and ϕ_2^{-1} with the inversion method used in our Lagrangian Push Forward (LPF) method [8].

1: $\forall t_i$ Initialize $\phi_1(t_i) = \phi_2(t_i) = \mathbf{Id}$.
2: **while** $\Delta E_{GN} > \epsilon_1$ **do**
3: Set $E_{old} = E_{new}$.
4: Compute $\phi_1(\mathbf{x}, 0.5)I$ and $\phi_2(\mathbf{x}, 0.5)J$.
5: Compute velocities from the symmetric Euler-Lagrange equations of 3.
6: Set $\|\boldsymbol{v}_1\| = \|\boldsymbol{v}_2\| = \min(\|\boldsymbol{v}_1\|, \|\boldsymbol{v}_2\|)$.
7: Update $\phi_1(0.5)$ and $\phi_2(0.5)$ by gradient descent such that, for $i = 1, 2$, $\phi_i(\mathbf{x}, 0.5) = \phi_i(\mathbf{x}, 0.5) + \lambda \boldsymbol{V}_i(\mathbf{x}, 0.5)$ where $\boldsymbol{V}(\mathbf{x}, 0.5) = \boldsymbol{v}(\phi_i(\mathbf{x}, 0.5))$ and λ is a gradient step length.
8: Starting at time 0.5 and going backwards toward 0, for all time points, t_i where $0 < t_i < 0.5$, update ϕ_1, ϕ_2 by gradient descent on the length of ϕ_1 and ϕ_2. Note that $\phi_i(0) = \mathbf{Id}$ and $\phi_i(0.5)$ does not change in this step.
9: Use the inversion method (below) to find ϕ_1^{-1} and ϕ_2^{-1} over all time.
10: Compute E_{new} from equation 3.
11: $\Delta E_{GN} = E_{old} - E_{new}$.
12: **end while**

Symmetry (guaranteed sub-pixel invertibility and algorithmic independence to input permutations) is built into GN and allows us to symmetrically match images to the degree that discrete diffeomorphisms are invertible. An example of a symmetric image registration when large deformations are present is shown in figure 3. Here, we use GN to find spatial correspondences by deforming a half C to a full C. We also illustrate GN for normalizing severely atrophied brains, some of which also suffer from the presence of lesions, in figure 4.

4 Discussion

A common problem with image normalization algorithms, in general, is asymmetry. Registering image I to J may not produce the same correspondences as

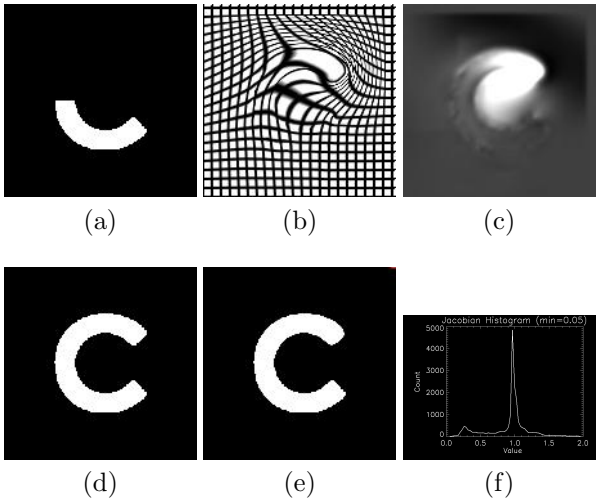

Fig. 3. The $\frac{1}{2}C$ (a) is registered to the full C (d). The grid of the deformation from (a) to (d) is shown in figure (b). The Jacobian of the transformation from C to $\frac{1}{2}C$ is in (c) while its histogram is in (f). The $\frac{1}{2}C$ to C result is in (e).

registering J to I. This problem has been addressed by methods that compute mappings in both directions. Thirion developed such an approach for Demons image registration [27]. Christensen's inverse consistent image registration (ICIR) [28] uses a similar idea. Both algorithms rely upon estimating a measure of "consistency", defined as the difference between the mapping from I to J and the mapping from J to I. Define $\mathbf{x}$ in image I, its displacement $\mathbf{u}(\mathbf{x})$ and their sum as $\mathbf{y} = \mathbf{x} + \mathbf{u}(\mathbf{x})$. Similarly, define $\mathbf{z}$ in image J and its displacement $\mathbf{w}(\mathbf{z})$. Consistency at $\mathbf{x}$ is $C(\mathbf{x}) = \|\mathbf{y} + \mathbf{w}(\mathbf{y}) - \mathbf{x}\| = \|\mathbf{u}(\mathbf{x}) + \mathbf{w}(\mathbf{y})\|$. Both algorithms attempt to minimize $C(\mathbf{x})$ and, similarly, $C(\mathbf{z})$. However, neither method guarantees the inverse's existence nor gives a well-defined numerical method for its computation.

Geodesic image normalization subsumes the above approaches by formulating the normalization process in space and time with a diffeomorphic parameterization. We do not have to "check" the consistency as (via Theorem 1) the consistency is guaranteed by the sub-pixel invertibility of ϕ_1 and ϕ_2 and the fact that these transformations may be composed together. Furthermore, our methods explicitly optimize these transformations in the large deformation space.

5 Conclusion

We explicitly optimize the length of ϕ, parameterized symmetrically by its components, ϕ_1, ϕ_2. Optimizing the length of a diffeomorphism is an alternative to finding a geodesic by solving the Euler equations [29]. Our method is shown

to satisfy the axioms of continuity, symmetry and unanimity. Satisfying these properties eliminates problems of algorithmic asymmetry. Finally, GN gives a robust estimate to geodesic distance that is invariant to which image, of a pair, is selected as template. Future work will focus on empirically demonstrating improved performance due to symmetrically parameterizing the large deformation image normalization problem.

References

1. C. Darwin, *Origin of Species*, John Murray: London, UK, 1856.
2. D. W. Thompson, *On Growth and Form*, Cambridge University Press, England, 1917.
3. A. M. Dale, B. Fischl, and M. I. Sereno, "Cortical surface-based analysis i: Segmentation and surface reconstruction," *Neuroimage*, vol. 9, no. 2, pp. 179–194, 1999.
4. P. Thompson and A. Toga, "A surface-based technique for warping 3-dimensional images of the brain," *IEEE Trans. Medical Imaging*, vol. 15, no. 4, pp. 402–417, 1996.
5. J. G. Csernansky, S. Joshi, L. Wang, J. W. Haller, M. Gado, J. P. Miller, U. Grenander, and M. I. Miller, "Hippocampal morphometry in schizophrenia by high dimensional brain mapping," *Proc. Natl. Acad. Sci. (USA)*, vol. 95, no. 19, pp. 11406–11411, 1998.
6. C. Studholme, V. Cardenas, R. Blumenfeld, N. Schuff, H. J. Rosen, B. Miller, and M. Weiner, "Deformation tensor morphometry of semantic dementia with quantitative validation," *Neuroimage*, vol. 21, no. 4, pp. 1387–1398, 2004.
7. M. I. Miller, M. F. Beg, C. Ceritoglu, and C. Stark, "Increasing the power of functional maps of the medial temporal lobe by using large deformation diffeomorphic metric mapping," *PNAS*, vol. 102, no. 27, pp. 9685–9690, 2005.
8. B. Avants, P. T. Schoenemann, and J. C. Gee, "Landmark and intensity-driven lagrangian frame diffeomorphic image registration: Application to structurally and functionally based inter-species comparison," *Medical Image Analysis*, vol. 10, pp. 397–412, 2006.
9. C. Yan, M. I. Miller, R. L. Winslow, and L. Younes, "Large deformation diffeomorphic metric mapping of vector fields," *tmi*, vol. 24, no. 9, pp. 1216–1230, 2005.
10. U. Grenander, *General Pattern Theory*, Oxford University Press, New York, 1993.
11. D. Mumford, "Pattern theory and vision," *Questions Matheematiques En Traitement Du Signal et de L'Image*, vol. 3, pp. 7–13, 1998.
12. F. Beg, M. Miller, A. Trouve, and L. Younes, "Computing large deformation metric mappings via geodesic flows of diffeomorphisms," *Int. J. Comp. Vision*, vol. 61, pp. 139–157, 2005.
13. A. Trouve, "Diffeomorphism groups and pattern matching in image analysis," *Intl. J. Comp. Vis.*, vol. 28, no. 3, pp. 213–221, 1998.
14. A. Trouve and L. Younes, "On a class of diffeomorphic matching problems in one dimension," *SIAM Journal on Control and Optimization*, vol. 39, no. 4, pp. 1112–1135, 2000.
15. M. Miller, A. Trouve, and L. Younes, "On the metrics and Euler-Lagrange equations of computational anatomy," *Annu. Rev. Biomed. Eng.*, vol. 4, pp. 375–405, 2002.

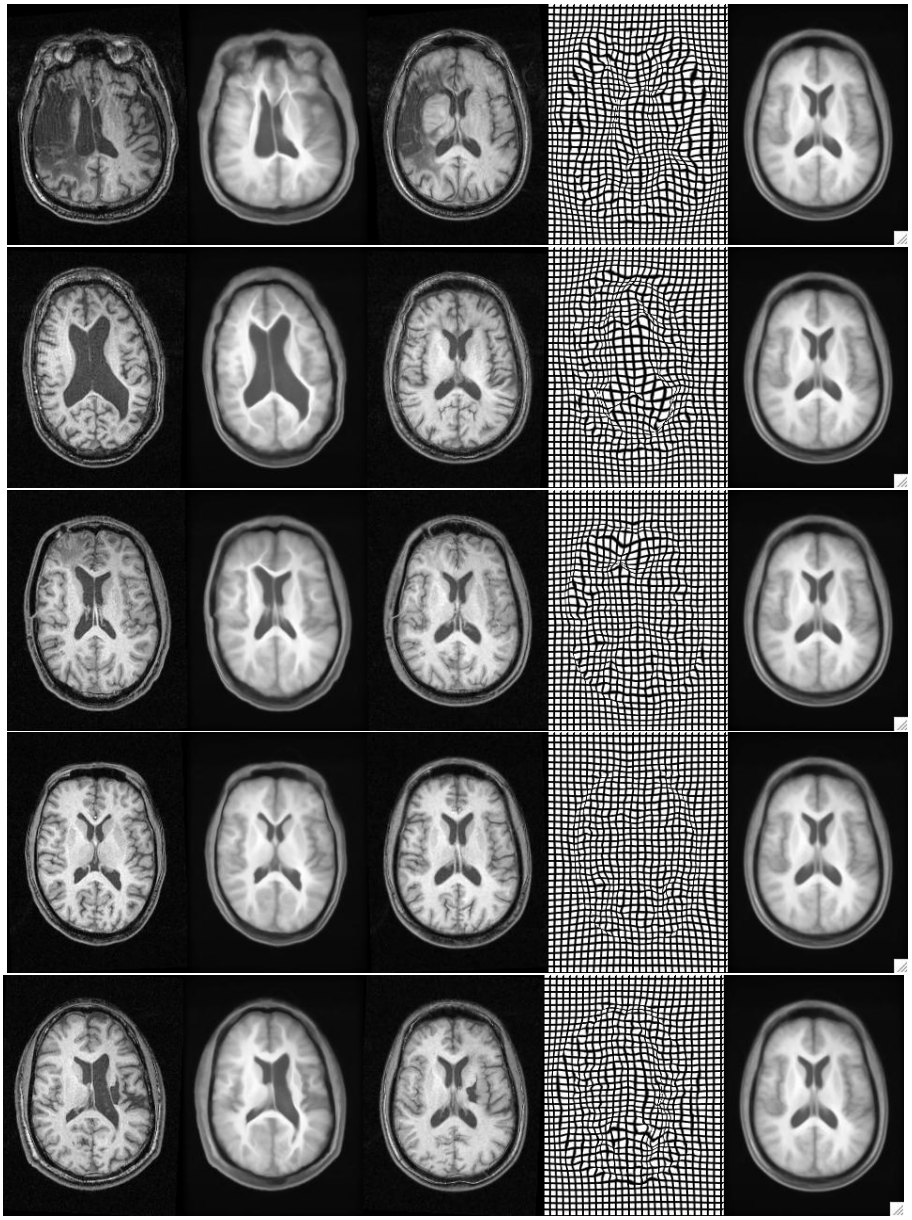

Fig. 4. We volumetrically map an average image template to a set of lesioned and/or atrophied brains using GN. The left column shows a slice of the original subject image. The second column shows the template mapped to the subject space. The center column shows the subject mapped to template space. The second to last column shows the grid deformation from template to subject. The final column shows the original template slice. Asymmetric methods do not perform as well for normalizing this dataset, particularly in the presence of difficult and unpredictable lesions.

16. V. I. Arnold, "Sur la gomtrie direntielle des groupes de lie de dimension innie et ses applications l'hydrodynamique des uides parfaits," *Ann. Inst. Fourier (Grenoble)*, vol. 16, no. 1, pp. 319–361, 1966.
17. S. Weinberger, "On the topological social choice model," *J. Econom. Theory*, vol. 115, no. 2, pp. 377–384, 2004.
18. V. I. Arnold, *Ordinary Differential Equations*, Springer-Verlag: Berlin, 1991.
19. J. Marsden and T. Ratiu, *Introduction to Mechanics and Symmetry*, Springer-Verlag: New York., 1999.
20. P. Dupuis, U. Grenander, and M. I. Miller, "Variational problems on flows of diffeomorphisms for image matching," *Quarterly of Applied Mathematics*, vol. 56, no. 3, pp. 587–600, 1998.
21. R. Schmid, "Infinite dimensional Lie groups with applications in mathematical physics," *Journal of Geometry and Symmetry in Physics*, vol. 1, pp. 1–67, 2004.
22. S. Joshi, B. Davis, M. Jomier, and G. Gerig, "Unbiased diffeomorphic atlas construction for computational anatomy," *Neuroimage*, vol. Suppl. 1, pp. S151–S160, September 2004.
23. B. Avants and J.C. Gee, "Geodesic estimation for large deformation anatomical shape and intensity averaging," *Neuroimage*, vol. Suppl. 1, pp. S139–150, 2004.
24. H. J. Johnson and G. E. Christensen, "Consistent landmark and intensity-based image registration," *IEEE Trans. Med. Imaging*, vol. 21, no. 5, pp. 450–461, 2002.
25. B. Avants, C. L. Epstein, and J. C. Gee, "Geodesic image interpolation: Parameterizing and interpolating spatiotemporal images," in *ICCV Workshop on Variational and Level Set Methods*, 2005, pp. 247–258.
26. B. Eckmann, "Social choice and topology," lecture notes, 2003.
27. J. Thirion, "Image matching as a diffusion process: an analogy with maxwell's demons," *Medical Image Analysis*, vol. 2, no. 3, pp. 243–260, 1998.
28. G. Christensen and H. Johnson, "Consistent image registration," *IEEE Transactions on Medical Imaging*, vol. 20, no. 7, pp. 568–582, 2001.
29. V. I. Arnold and B. A. Khesin, "Topological methods in hydrodynamics," *Ann. Rev. Fluid Mech.*, vol. 24, pp. 145–166, 1992.